

The colour of the Deep *ROSAT* X-ray sky fluctuations

M.T. Ceballos^{1,2}, X. Barcons¹ and F.J. Carrera¹

¹ *Instituto de Física de Cantabria (Consejo Superior de Investigaciones Científicas - Universidad de Cantabria), 39005 Santander, Spain*

² *Departamento de Física Moderna, Universidad de Cantabria, 39005 Santander, Spain*

24 November 2018

ABSTRACT

We have carried out a fluctuation analysis in four bands (R4, R5, R6 and R7 corresponding to 0.44–1.01 keV, 0.56–1.21 keV, 0.73–1.56 keV and to 1.05–2.04 keV respectively) of two very deep *ROSAT* PSPC observations in directions where the galactic HI column is minimal. This has enabled us to study the average spectrum of the sources contributing to 0.5–2 keV fluxes $\sim 10^{-15} \text{erg cm}^{-2} \text{s}^{-1}$. The best fit spectral energy index for the average faint source spectrum, $\alpha = 0.95_{-0.15}^{+0.10}$, is still steeper than the one measured for the extragalactic XRB at these energies $\alpha \sim 0.4 - 0.7$, but flatter than the typical AGN spectral index $\alpha \sim 1 - 1.5$. This result has allowed us to constrain the existence of a population of sources harder than the AGNs contributing to the source counts at these fluxes. We find that a population of X-ray sources with energy spectral index $\alpha \sim 0.4 - 0.6$ would contribute (30 ± 20) per cent to the source counts at these fluxes if the rest of them are AGNs with energy spectral index $\alpha \sim 1.2$.

Key words: X-rays: general - diffuse radiation - galaxies: active - methods: statistical

1 INTRODUCTION

The existence of a population, different to the AGNs, of faint sources with hard X-ray spectra has been proposed in several works. Hasinger et al. (1993) considered these sources as a possible explanation for the discrepancy between the source number counts found in their analysis and the number counts predicted by the integration of models for the AGN X-ray luminosity function at fluxes $S \sim 2.5 \times 10^{-15} \text{erg cm}^{-2} \text{s}^{-1}$. The idea is also supported by the tendency shown by the sources in their sample to be harder at fainter fluxes (see also Vikhlinin et al. 1995 for further evidence on this hardening).

Moreover, should these sources exist they could help to solve the spectral paradox concerning the origin of the soft X-ray background: the fact that while the spectral shape of the cosmic background at energies $\gtrsim 0.8$ keV is consistent with an energy spectral index $\alpha \sim 0.4$ (Gendreau et al. 1995) or $\alpha \lesssim 0.6$ in the 0.5–2 keV band (Barber & Warwick 1994, Chen et al. 1994), the mean spectral index of the Broad Line AGNs in the 0.5–2 keV band, which are thought to be its main contributors (Shanks et al. 1991, Boyle et al. 1994, Hasinger et al. 1993), is $\gtrsim 1.0$.

Recent work by Romero-Colmenero et al. (1996) and Griffiths et al. (1996) has suggested that this new population might be dominated by Narrow Emission Line Galaxies having a mean spectral slope of $\alpha \sim 0.4$. The ratio between the number density of these galaxies and the Broad Line

AGNs is found to increase towards fainter fluxes pointing to these sources as important contributors to the extragalactic X-ray background at soft energies (< 2 keV).

In this work we have carried out an analysis of the sky fluctuations in four spectral bands of two deep *ROSAT* observations. This analysis has allowed us to constrain the summed spectral shape of the sources contributing at fluxes where this technique is sensitive ($\sim 10^{-15} \text{erg cm}^{-2} \text{s}^{-1}$, 0.5–2 keV), below the direct source detection limit. Moreover, we have estimated the fraction of the total number of sources represented by any population of sources harder than the AGNs.

In section 2 we give a brief description of the data used in the analysis. In section 3 we explain how we used the P(D) analysis technique to derive the spectral shape of the sources dominating the fluctuations. Finally in Section 4 we discuss the implications of our study and the fraction of sources harder than the AGNs compatible with fluctuations results.

2 DATA

The *ROSAT* PSPC data used in the analysis are listed in Table 1. Some of the images were extracted from the UK Deep Survey (Branduardi-Raymont et al. 1994) and are labelled by UKDS in the table. The other ones - those beginning with LHDS - come from the observations of the Lock-

arXiv:astro-ph/9611029v1 5 Nov 1996

Table 1. Data images from the Deep surveys

| Image Name | Channels | Exposure Time (seconds) | Clean Time (seconds) | Galactic HI Column Density (cm^{-2}) | Mean counts ($\text{counts arcmin}^{-2}$) |
|------------|-----------|-------------------------|----------------------|---|---|
| UKDS-R4 | 52 - 69 | 73311 | 69525 | 6.5×10^{19} | 6.64 ± 0.12 |
| UKDS-R5 | 70 - 90 | 73311 | 69525 | 6.5×10^{19} | 4.91 ± 0.12 |
| UKDS-R6 | 91 - 131 | 73311 | 69525 | 6.5×10^{19} | 4.64 ± 0.15 |
| UKDS-R7 | 132 - 201 | 73311 | 69525 | 6.5×10^{19} | 2.88 ± 0.10 |
| UKDS-HARD | 40 - 200 | 73311 | 69525 | 6.5×10^{19} | 25.19 ± 0.41 |
| LHDS-R4 | 52 - 69 | 143700 | 93129 | 6.0×10^{19} | 11.48 ± 0.13 |
| LHDS-R5 | 70 - 90 | 143700 | 93129 | 6.0×10^{19} | 6.73 ± 0.14 |
| LHDS-R6 | 91 - 131 | 143700 | 93129 | 6.0×10^{19} | 5.98 ± 0.16 |
| LHDS-R7 | 132 - 201 | 143700 | 93129 | 6.0×10^{19} | 3.91 ± 0.12 |
| LHDS-HARD | 40 - 200 | 143700 | 93129 | 6.0×10^{19} | 36.09 ± 0.42 |

man Hole (Hasinger et al. 1993). These two surveys were selected due to their low galactic absorbing column and their high exposure time. At such a low galactic HI absorbing columns, observations above 0.5 keV are insensitive to the precise value of the HI column density. The event files were extracted from the LEDAS archive and were reduced using the standard package ASTERIX.

Both the original exposure time and the clean time are listed for each image. Clean time refers to the remaining periods after suppressing the intervals where the mean PSPC count rate was excessively high (contamination by geocoronal or auroral backgrounds, solar scattering, unfavourable viewing conditions). We have also rejected data intervals where severe particle background contamination could not be modelled accurately (Master Veto Rate > 170) (see Snowden et al. 1994 and references therein).

The R4, R5, R6 and R7 bands (as defined by Snowden et al. 1994) correspond to energies (10 per cent of peak response) ~ 0.44 to ~ 1.01 keV, ~ 0.56 to ~ 1.21 keV, ~ 0.73 to ~ 1.56 keV and to ~ 1.05 to 2.04 keV respectively and consequently they span all of the 0.5-2 keV energy range. Moreover, they do not cover the softer energies (0.1 - 0.4 keV) where the internal background as well as the contamination produced by the Galactic component (both in emission and absorption) of the diffuse background are more important. We also analysed the images called HARD in the table to compare our results with those obtained by previous works (Barcons et al. 1994, Hasinger et al. 1993).

Only the inner part (squares of 30×30 arcmin) of the PSPC field of view was used for our analysis in order to reduce systematic effects and uncertainties such as vignetting and variations of the Point Spread Function (PSF). The PSF was modelled as a two dimensional Gaussian with dispersion 10 arcsec which corresponds to the measured PSF for on-axis sources (Hasinger et al. 1992). Finally the images were extracted in 1 arcmin² pixels so that the specific shape of the PSF is almost irrelevant and to avoid the pixel intensities being correlated. That ensures that our statistical analysis of the distribution of the fluctuations, based on the assumption that each intensity is an independent measurement, is a good approximation.

3 ANALYSIS

First used in radio astronomy (Scheuer 1957, Condon 1974) the fluctuations analysis technique (also called the P(D) analysis) has been lately used in X-ray astronomy to obtain the number of sources per flux interval (the $n(S)$ curve) below the direct source detection threshold (Shafer 1983 for *HEAO-1* A2 data, Barcons & Fabian 1990, for *Einstein Observatory* IPC images; Barcons et al. 1994 for *ROSAT* images; Butcher et al. 1996 for *Ginga* pointings).

The underlying idea is that the shape of the distribution of intensities is sensitive to fluxes down where there is about one source per beam. Extrapolating previous fits to the $n(S)$ curve (Branduardi-Raymont et al. 1994, Hasinger et al. 1993) it is found that the lowest flux where this technique is applicable (one source per beam level) is $\sim 10^{-16} \text{ erg cm}^{-2} \text{ s}^{-1}$. However, one has to take into account that the noise in the *ROSAT* PSPC observations, even with a pixel of 1 arcmin², is dominated by Poisson photon counting noise. It then happens that this noise is equivalent to a flux $\sim 10^{-15} \text{ erg cm}^{-2} \text{ s}^{-1}$ much larger than the one source per beam level. In this paper we adopt the conservative view (as in Barcons et al. 1994) that the fluctuation analysis can hardly say anything below fluxes equivalent to the photon counting noise. Therefore we expect our analysis to be sensitive from $1 - 2 \times 10^{-15} \text{ erg cm}^{-2} \text{ s}^{-1}$ up to $5 - 6 \times 10^{-15} \text{ erg cm}^{-2} \text{ s}^{-1}$ which is approximately the flux where the intensity histograms rise significantly, proceeding from the high-intensity tail downwards. Pixels with intensities larger than these fluxes will typically contribute only the highest intensity bin in the P(D) curve which we have selected to have 15 pixels (see below).

The observed intensity distribution is fitted with a theoretical model which basically includes the PSF, the differential source counts function $n(S)$ and the photon-counting noise. Detailed descriptions of this technique can be found in Scheuer (1974), Fabian (1975), Shafer (1983), Warwick & Stewart (1989), Barcons (1992).

We have carried out a fluctuation analysis in the four bands mentioned above (R4, R5, R6 and R7). In addition to obtaining the source counts at fluxes below the detection threshold, this four-band analysis has allowed us to constrain the average spectrum of the sources existing at these low fluxes. With only one spectral band the change of the

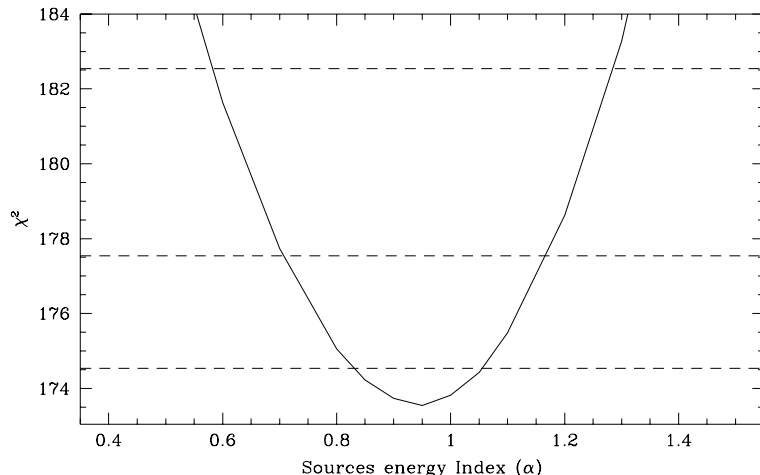


Figure 1. χ^2 as a function of the index α taking K and γ as uninteresting parameters. Also represented as horizontal lines are the 1σ , 2σ and 3σ confidence levels (from bottom to top).

spectral index of the sources just results in a rescaling of the normalization factor in the $n(S)$ curve.

We parametrised the $n(S)$ curve (in the 0.5-2 keV band) as a broken power law with an Euclidean slope above the break:

$$n(S) = \begin{cases} \frac{K}{S_B} \left(\frac{S}{S_B}\right)^{-\gamma} & S < S_B \\ \frac{K}{S_B} \left(\frac{S}{S_B}\right)^{-2.5} & S > S_B \end{cases} \quad (1)$$

where the fluxes also refer to the 0.5-2 keV band. The break flux (S_B) is taken to be 2.2×10^{-14} erg cm $^{-2}$ s $^{-1}$ (Hasinger et al. 1993, Branduardi-Raymont et al. 1994) although its exact value is not very important here due to the fact that we are working at fluxes well below this flux break. Both the normalization and the slope below the break (γ) will be obtained from the fitting to the intensity distribution curve. Assuming that the spectra of all the sources are described with a power law model with the same ‘average’ energy index α (i.e. there is no segregation in flux), the fluxes S and S_B can be translated to each band taking this index into account. The normalization K of the curve $n(S)$ is then the same in all the spectral bands.

Once the intensity distribution from the source counts is derived we add a constant (P_m) to all intensities in such a way that the mean intensity matches the measured one (I_m). Finally the distribution in counts per pixel is derived by considering Poisson photon-counting noise on this distribution.

However due to the limited amount of pixels and the distribution of intensities, the mean total count number per pixel (I_m) is poorly determined (see Table 1). To take into account this effect we let the Poissonian mean vary and add a new term to the χ^2 obtained from the parameters of the sources. This is considered as a new uninteresting parameter to be fitted by the model. Then we minimize χ^2 with respect to P_m :

$$\chi^2(K, \gamma, \alpha) = \text{MIN}_{P_m} \left[\chi^2(K, \gamma, \alpha, P_m) \right. \\ \left. + \left(\frac{I_m - P_m - S_m}{\sigma} \right)^2 \right] \quad (2)$$

where σ is the standard error in the measurement of I_m , S_m is the average intensity contributed by the sources and α is the spectral energy index of the sources.

In this way those sets of parameters (K , γ , α , P_m) with a value of P_m quite far from $I_m - S_m$ give rise to high values of the additional term in χ^2 and therefore are less likely. To compare this approach with previous work, we note that Barcons et al. (1994) allowed the average count per pixel to vary freely between the measured $\pm 2\sigma$ interval, but without adding the extra term in the χ^2 . A similar computation was performed by Hasinger et al. (1993) allowing for a 5 per cent variation in the mean. We believe that the approach we use here is more robust, since it takes into account the measured value of the mean with its uncertainties as an extra observational parameter to be fitted by the model.

The histograms obtained are rebinned to have at least 15 pixels falling in each bin since otherwise χ^2 statistics would hardly be applicable. This is due to the fact that we estimate the dispersion in the distribution of pixel intensities based on gaussian statistics on the number of pixels per bin which therefore has to be large enough. Then a grid of χ^2 is produced (one value for each set of three parameters K , γ , α) to find the best-fitting parameters of the $n(S)$ curve and also the confidence contours.

We first applied this analysis to the HARD bands (channels 40-200) assuming $\alpha = 1.0$ in order to compare it with previous works. We found the minimum χ^2 in $\gamma = 1.88^{+0.28}_{-0.15}$ (2σ errors) for the UKDS-HARD band and in $\gamma = 2.09^{+0.08}_{-0.25}$, (2σ errors) for the LHDS-HARD band which closely reproduce the best fits found by Barcons et al. (1994) and Hasinger et al. (1993) respectively.

Then we applied the same process to each of our eight images (UKDS-R4, UKDS-R5, UKDS-R6, UKDS-R7, LHDS-R4, LHDS-R5, LHDS-R6 and LHDS-R7) for several values of α ranging from $\alpha = 0.4$ to $\alpha = 1.5$ with the aim of measuring the average spectrum of the sources dominating

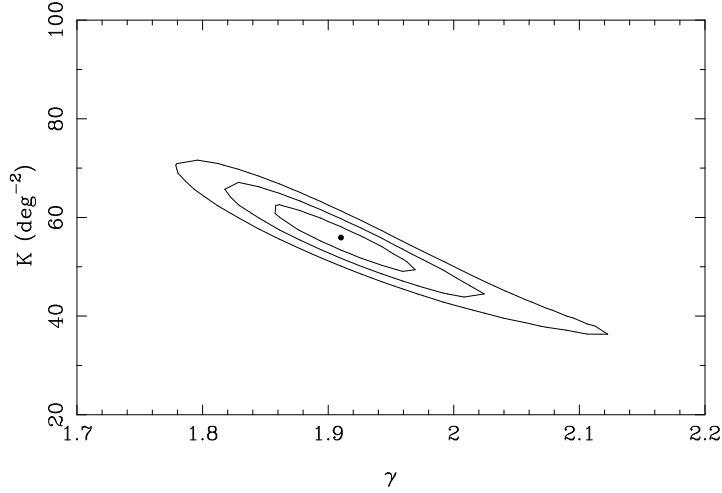


Figure 2. Confidence contours for 1σ (innermost curve), 2σ , and 3σ (outermost curve) levels in the (K, γ) parameter space for the simultaneous fit to the UKDS and LHDS Deep Surveys and $\alpha=0.95$. The point represents the best fit.

the fluctuations. Since we want to fit all the images simultaneously we minimized the sum of the χ^2 in K and γ , for each α :

$$\begin{aligned} \chi_{tot}^2(K, \gamma, \alpha) = & \chi_{UKDS-R4}^2(K, \gamma, \alpha) + \chi_{UKDS-R5}^2(K, \gamma, \alpha) \\ & + \chi_{UKDS-R6}^2(K, \gamma, \alpha) + \chi_{UKDS-R7}^2(K, \gamma, \alpha) \\ & + \chi_{LHDS-R4}^2(K, \gamma, \alpha) + \chi_{LHDS-R5}^2(K, \gamma, \alpha) \\ & + \chi_{LHDS-R6}^2(K, \gamma, \alpha) + \chi_{LHDS-R7}^2(K, \gamma, \alpha) \end{aligned} \quad (3)$$

$$\chi^2(\alpha) = \text{MIN}_{K, \gamma} [\chi_{tot}^2(K, \gamma, \alpha)] \quad (4)$$

The variation of χ^2 for the joint fit with UKDS and LHDS Deep surveys as a function of the spectral energy index is shown in Fig. 1. The minimum is reached at $\alpha = 0.95_{-0.15}^{+0.10}$ (1σ errors) with a minimum $\chi^2 = 173.54$ for 112 degrees of freedom. In this case $K = 55.92_{-4.30}^{+4.13} \text{ deg}^{-2}$ and $\gamma = 1.91_{-0.04}^{+0.03}$ which is consistent at 1σ significance level with previous fits in the HARD (0.5-2 keV) band.

Fig. 2 shows the (K, γ) parameter space for this simultaneous fit to the UKDS and LHDS images with $\alpha = 0.95$ (best fit). The point is the best fit and the contours correspond to 1σ , 2σ , and 3σ significance levels.

If fitted separately UKDS and LHDS images give different best-fits for the sources energy spectral index and for the parameters of the $n(S)$ curve. While the fit to UKDS images shows a tendency towards high spectral energy indices ($\alpha_{best\ fit}(UKDS) \sim 1.1$) the best-fitting point for the four bands of the LHDS image is $\alpha_{best\ fit}(LHDS) \sim 0.8$. Although it might be an interesting result to establish that the slightly fainter sources dominating the LHDS fluctuations would have harder spectra than the UKDS ones, the difference in spectral indices between both fits is not significant (certainly less than 2 sigma). Since, in addition, both best fit values are also within the 1 sigma range of the spectral energy index measured by taking both images, we interpret this difference as being purely statistical.

4 DISCUSSION

We have carried out a fluctuations analysis on four different bands of two *ROSAT* PSPC deep surveys simultaneously. This has enabled us to obtain an energy index for the average spectrum of the sources contributing to fluxes where this analysis is sensitive (0.5-2 keV fluxes around and below $\sim 10^{-15} \text{ erg cm}^{-2} \text{ s}^{-1}$).

The best-fitting spectral slope for the sources has been found to be $\alpha = 0.95_{-0.15}^{+0.10}$ which does not result in a very significant flattening of the mean spectral index with regard to that of the sources (AGN) known to dominate the source counts at higher fluxes ($\alpha \sim 1.0 - 1.5$). This seems to be in contrast with the tendency exhibited by the X-ray sources found in previous analyses of *ROSAT* PSPC images, according to which fainter sources have harder spectra (Hasinger et al. 1993, Vikhlinin et al. 1995).

Since the spectral slope we derive in our analysis is an average spectrum, we tested the possibility of the existence of two different populations of sources contributing to the source counts at the interval of fluxes we are dealing with (see section 2). One of these populations would be made up by the AGNs ($\alpha \sim 1.0 - 1.5$, say, $\alpha = 1.2$) and the other one by sources with harder spectra. We assigned to this last population a fraction f_0 of the total number of sources at a representative flux, $S \sim 10^{-15} \text{ erg cm}^{-2} \text{ s}^{-1}$ and an energy spectral index α_0 . We then calculated the total count rate that both classes of sources would produce in each spectral band for a given pair of values (α_0, f_0) .

$$R_i^S = f_0 (R_i)_{\alpha_0}^S + (1 - f_0) (R_i)_{\alpha=1.2}^S \quad (5)$$

with $i = 4, 5, 6, 7$ for R4, R5, R6 and R7 bands respectively.

In this equation R_i gives the count rate produced by the corresponding class of sources at flux S in the i band and was calculated with the X-ray spectral analysis package XSPEC assuming power law models. If now we assume that the whole population of sources has the same spectrum, we can obtain this ‘average’ energy spectral index (α_i) able to reproduce the count rate in each band, R_i .

As we have previously calculated the value of the χ^2 re-

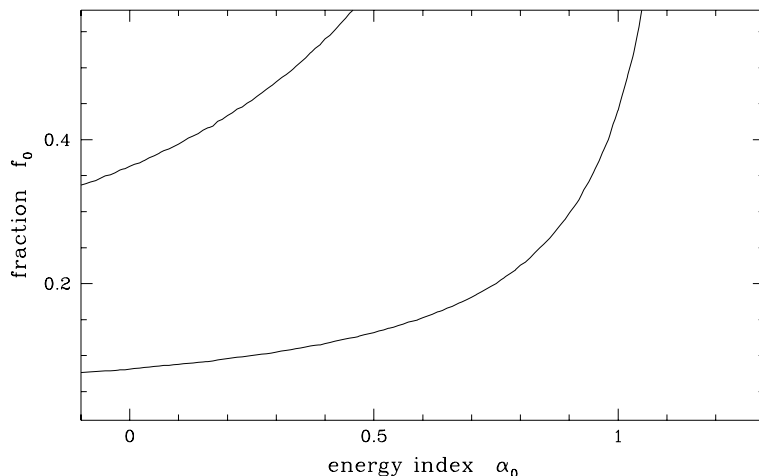


Figure 3. Permitted region for a hypothetical harder population in the f_0 , α_0 parameter space (see text for details). The lines encompass the 1σ confidence interval.

sulting from the $P(D)$ analysis for each set of parameters α , K , γ in each spectral band (see equation 3), we can calculate the total χ^2 for each pair α_0 , f_0 :

$$\chi^2(\alpha_0, f_0) = \text{MIN}_{K,\gamma} \sum_{i,j} \chi_{i,j}^2(\alpha_i, K, \gamma) \quad (6)$$

where $i = 4, 5, 6, 7$ as before, and $j = 1$ for the UK Deep Survey images and $j = 2$ for the Lockman Hole ones.

In Fig. 3 we show the (α_0, f_0) parameter space resulting from this calculation, where the lines limit the permitted region from the 1σ confidence interval.

The conclusion that can be extracted from this analysis is that provided this second population exists and is made up of some type of galaxies, for which an energy spectral index $\alpha_0 = 0.4-0.6$ is being found (Romero-Colmenero et al. 1996, Carballo et al. 1995), these sources would constitute $\sim (30 \pm 20)$ per cent of the source counts at $\sim 10^{-15} \text{ erg cm}^{-2} \text{ s}^{-1}$.

Yet, with the data we have it is not possible to distinguish whether both populations are segregated in flux (fainter sources with harder spectra) or on the contrary, there is a complete mixture through all the interval of fluxes we have been considering here. Moreover far from providing the solution to the X-ray background spectral paradox this analysis has confirmed the tendency already known at higher fluxes: the sources seem to be too soft to account for the spectrum of the cosmic X-ray radiation at low energies.

This research has made use of data obtained from the Leicester Database and Archive Service at the Department of Physics and Astronomy, Leicester University, UK. Partial financial support for this work was provided by the DGICYT under project PB92-0501.

REFERENCES

- arber C.R., Warwick R.S., 1994, MNRAS, 267, 270
 arcons X., 1992, ApJ, 396, 460
 arcons X., Branduardi-Raymont G., Warwick R.S., Fabian A.C., Mason K.O., McHardy I.M., Rowan-Robinson M., 1994, MNRAS, 268, 833
 arcons X., Fabian A.C., 1990, MNRAS, 243, 366
 oyle B.J., Shanks T., Georgantopoulos I., Stewart G.C., Griffiths R.E., 1994, MNRAS, 271, 639
 randuardi-Raymont G. et al., 1994, MNRAS, 270, 947
 utcher et al. 1996, MNRAS, submitted
 arballo R., Warwick R.S., Barcons X., González-Serrano J.I., Barber C.R., Martínez-González E., Pérez-Fournon I., Burgos J., 1995, MNRAS, 277, 1312
 hen L.-W., Fabian A.C., Warwick R.S., Branduardi-Raymont G., Barber C.R., 1994, MNRAS, 266, 846
 ondon J.J., 1974, ApJ, 188, 279
 abian A.C., 1975, MNRAS, 172, 149
 endreau K.C. et al. 1995, PASJ, 47, L5
 r Griffiths R.E., Della Ceca R., Georgantopoulos I., Boyle B.J., Stewart G.C., Shanks T., Fruscione A., 1996, MNRAS, 281, 71
 amilton T.T., Helfand D.J., 1987, ApJ, 318, 93
 asinger G., Burg R., Giacconi R., Hartner G., Schmidt M., Trümper J., Zamorani G., 1993, A&A, 275, 1
 asinger G., Turner T.J., George I.M., Boess G., 1992, NASA/GSFC OGIP Calibration Memo CAL/ROS/92-001
 omero-Colmenero E., Branduardi-Raymont G., Carrera F.J., Jones L.R., Mason K.O., McHardy I.M., Mittaz J.P.D., 1996, MNRAS, 282, 94
 cheuer P.A.G., 1957, Proc. Camb. Phil. Soc., 53, 764
 cheuer P.A.G., 1974, MNRAS, 166, 329
 hafer R.A., 1983, PhD thesis, University of Maryland
 hanks T., Georgantopoulos I., Stewart G.C., Pounds K.A., Boyle B.J., Griffiths R.E., 1991, Nat, 353, 315
 nowden S.L., McCammon D., Burrows D.N., Mendenhall J.A., 1994, ApJ, 424, 714
 ikhlinin A., Forman W., Jones C., Murray S., 1995, ApJ, 451, 564
 arwick R.S., Stewart G.C., 1989, in Hunt J., Battrick B., eds, Proc. 23rd ESLAB Symp. on Two Topics in X-ray Astronomy. ESA, Noordwijk, p. 727

This paper has been produced using the Royal Astronomical Society/Blackwell Science \LaTeX style file.